

Spectrum-Compact Signals

A Suitable Option for Future GNSS

VALERY P. IPATOV, BORIS V. SHEBSHAEVICH

THE RUSSIAN INSTITUTE OF RADIONAVIGATION AND TIME

As the number of GNSS satellites on orbit and signal transmissions grow, out-of-band emissions and in-band RF noise also increase, raising issues of signal compatibility. One solution might be to use more spectrum-efficient signal structures. In this article, the authors explore the use of minimum shift keying as an alternative to current GNSS signal designs.

In the early stages of developing space-based radionavigation, the spectrum compactness of ranging signals was not proclaimed among the material priorities. Conventional bi-phase shift keying (BPSK) modulations, although they consume a rather large amount of spectrum, were adopted as the basis for both GPS and GLONASS signals.

Later developments, such as the modernized civil GPS L1-band (L1C) and military (M-code) signals as well as some signals of Galileo and Compass/BeiDou-2, modified the plain BPSK a bit to take a form of binary offset carrier (BOC) modulation, which again is in no way bandwidth-efficient.

In the meantime, scenarios arose in which the penetration of GNSS signals into neighboring bands allocated to other systems appears to be tangibly harmful. One example of this sort is the collision between L1 GLONASS signals and an International Telecommunication Union (ITU)

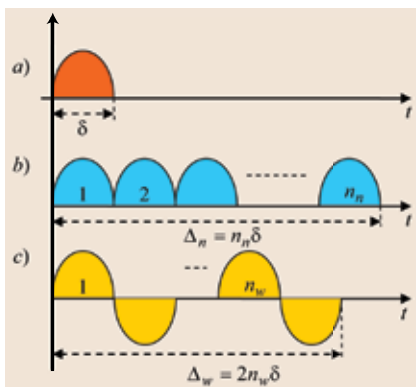


FIGURE 1 Microchip (a), narrow-band component chip (b), and wideband BOC-like component chip (c)

requirement to keep quite a low level of any side power flux within the radio astronomy window at 1610.6–1613.8 MHz.

The trouble here is that the power amplifier of a standard satellite transmitter does not tolerate amplitude modulation; so, signal prefiltering is not an option. Currently the attempts are being undertaken to solve the problem by post-amplifier band rejection, compromising the transmitter energy output and mass-dimension characteristics.

Similar challenges may be expected all the more in the future with the anticipated advances of satellite radio-navigation into new frequency bands, e.g. C-band. Attention to this possibility has recently been drawn in the articles by J.A. Avila-Rodriguez *et alia* and A. Schmitz-Peiffer *et alia* (see Additional Resources).

A radical way to organize navigation signals with a minimum out-of-band emission would be to replace traditional BPSK with some continuous-phase modulation (CPM), such as minimal shift keying (MSK) or one of its numerous enhanced analogs. Smooth changes in the complex amplitude of a CPM signal result in a very compact spectrum combined with the absence of amplitude modulation.

Owing to this characteristic, employing a CPM design in future GNSS signals could make it unnecessary to apply any post-amplifier rejection within the forbidden frequency range, or, at least, if a stop-band filter cannot be completely excluded, its implementation may turn

out not that demanding. Similar ideas have already been put forward in the articles mentioned earlier and also in the article by V. Ipatov and B. Shebshavich referenced in Additional Resources.

Of course, the bandwidth economy inherent to CPM is obtained at the cost of potentially compromising some other performance characteristics. Indeed, removal of high-frequency spectral components principally reduces root-mean-square signal bandwidth, thereby increasing the theoretically achievable noise error of the signal time-of-arrival estimate. Equally, one can expect degradation of multipath resistance again due to spectrum concentration within the narrower band.

In the sections to follow, however, we demonstrate that allowing for a limited bandwidth of the receiver frequency-selective circuits with preference to CPM modulation rather than BPSK often means either insignificant deterioration of these performance characteristics or even their improvement.

One more disputable issue is a way of aggregating two subsignals differing in bandwidth: narrowband (or civil) and wideband ones, into a united signal free of amplitude modulation. Creating this kind of combined signal does not present any difficulty if the modulation is BPSK or BOC, as takes place in GPS, Galileo, GLONASS, and other systems, where each of the subsignals modulates its own quadrature carrier component. As amplitude modulation does not occur in quadrature components and they are phase-shifted by $\pi/2$ to each other, no amplitude modulation appears in the resulting signal either.

Replacement of BPSK with the CPM means that the ranging signal elements — chips — are not rectangular any more, and each of subsignals becomes amplitude-modulated. In the next section we describe how to construct subsignal chips in order to come to the amplitude-modulation-free overall signal incorporating both subsignals.

As long as various versions of spectrally efficient modulation exist and our goal is just to uncover their common potential merits stemming from

the complex amplitude continuity, we can reasonably limit ourselves here to the simplest CPM mode, namely MSK. Further complications of CPM, particularly making continuous phase derivatives along with the current phase itself, can lead to even greater spectrum compactness.

Possible Structure of an MSK-Based Satellite Signal

As is well known (see, for example, the textbooks by J. Proakis or B. Sklar cited in Additional Resources), the MSK is just a modified version of the offset quadrature phase shift keying (OQPSK). In conventional OQPSK, streams of rectangular elementary symbols (chips in our case) of two quadrature branches are time-shifted to each other by a half symbol length. To convert OQPSK to MSK we only need to replace a rectangular chip with one having the shape of sine half-wave of the same duration.

Due to a mutual time shift of quadrature streams, a change of chip polarity caused by ranging coding in one branch occurs when the other branch chip passes its maximum. As a result of the smoothness of a half-sine chip, the overall signal comprising both branches has no phase jumps. Moreover, the half-sine chip shape provides amplitude constancy of the overall signal.

To roughly assess the spectral saving of a modulation and its share of out-of-band emissions, one can resort to the 99 percent bandwidth, $W_{0.99}$, which is a frequency span containing 99 percent of the total emitted signal power. For BPSK with chip length $\Delta W_{0.99} \approx 20/\Delta$, which is 10 times larger compared to the traditional figure $2/\Delta$, estimating the bandwidth by the space between first spectral zeros. In contrast to this, for an MSK modulation with the same chip length $W_{0.99} \approx 2.4/\Delta$, meaning more than an eightfold economy in the bandwidth actually occupied.

Let us base our further consideration on the premise that a future GNSS signal is to succeed the existing one in combining two (public and special) accuracy scales, meaning that it has to contain both narrowband (long-chip) and wide-

band (short-chip) components. At the same time, we can readily see from the previous discussion that, in order to implement an MSK discrete signal, the chips in both quadrature branches should be half-sines of the identical duration.

To reconcile these contradictions we propose to build both long-chip and short-chip components using universal short elements or microchips of duration δ (Figure 1a). Then a civil (narrowband) component chip of duration $\Delta_n = n_n \delta$ is a series of n_n microchips of the same polarity (Figure 1b), while a wideband component chip of duration Δ_w can be either a microchip itself ($\Delta_w = \delta$, Figure 1a) or a train of n_w pairs of sign-alternating microchips ($\Delta_w = 2n_w \delta$, Figure 1c). The latter option corresponds to the implementation of the BOC-modulation mode through MSK, which can be used to partly separate civil and special components spectra.

To come to the resulting MSK signal the two components constructed in this way should just be used in quadrature, that is, modulating in phase (I) and in quadrature (Q) carrier waves. In so doing, one of them has to be in a preliminary fashion half-microchip-shifted against the second, as is shown in Figure 2 for the case $n_n = 4$, $n_w = 1$.

An important comment to the suggested construction of a narrowband component: the simplest low-cost receiver has no need to reproduce the exact shape of chip of Figure 1b in a correlator reference. Instead, a conventional rectangular chip of length Δ_n could be used at the price of an energy loss of $\pi^2/8$, that is, about 0.9 decibel. In other words, if some day the GPS civil signal was switched to the proposed MSK modulation mode without changing ranging code, all existing commercial receivers would survive although suffering from the signal-to-noise (SNR) penalty as described.

In a rather immediate manner one can derive the expression for the power spectrum density $\tilde{G}(f)$ of the complete signal thus obtained, where a microchip serves as a wideband component chip. Being normalized to a total mean power it appears thus:

$$\tilde{G}(f) = \frac{4\delta}{\pi^2} \left| \frac{1}{[1 - (2f\delta)^2] \tan \pi f \delta} \right|^2 \left[\sin^2(\pi f \delta) + \frac{\sin^2(n_n \pi f \delta)}{n_n} \right] \quad (1)$$

Calculated from this equation, Figure 3 presents the power spectrum of a complete MSK-signal having components of chip durations Δ_n and Δ_w , the same as for GPS C/A and P codes: $n_n = 10$, $\Delta_n = 10\delta = 1/f_c = \Delta$, $\Delta_w = \delta$, $f_c = 1.023$ MHz. Also, in this figure the total normalized power spectrum of both GPS signals

$$\tilde{G}_{\text{GPS}}(f) = \frac{\delta}{2} \left(\frac{\sin \pi f \delta}{\pi f \delta} \right)^2 + \frac{\Delta}{2} \left(\frac{\sin \pi f \Delta}{\pi f \Delta} \right)^2 \quad (2)$$

is shown.

From a comparison of the curves two key inferences follow:

- Despite presence of the 10 MHz-distant spikes in MSK signal spectrum, deep and rather broad notches exist in between. The first of them can be aligned with the radio astronomy window — for example, by a proper carrier choice within an assigned L1 band (1592.9–1610 MHz),

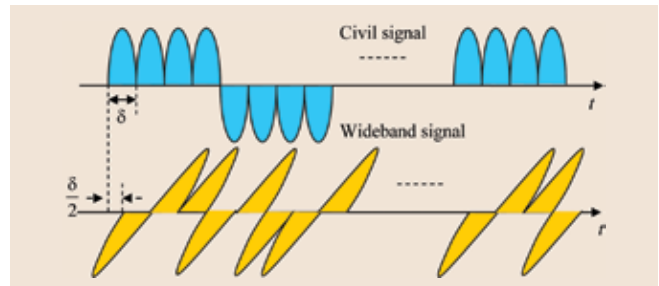


FIGURE 2 Combining civil and wideband components into an MSK signal

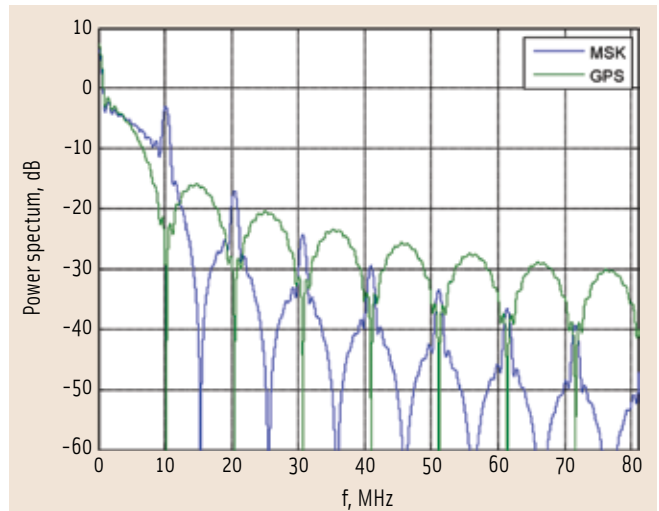


FIGURE 3 Total power spectrum of MSK type signal against its GPS analog

allowing a substantial reduction of GLONASS emissions penetrating into it.

- Maximum out-of-band emission for the MSK modulation mode drops with frequency much faster than for legacy BPSK GPS signals, which can be valuable from the electromagnetic compatibility point of view.

In support of this last thesis, calculation of the 99 percent bandwidth comprising both subsignals for the MSK modulation format results in $W_{0.99} \approx 2.3/\delta \approx 23$ MHz, if long and short chip durations are the same as in the GPS C/A and P codes. For the overall spectrum of the latter, a similar figure would be $W_{0.99} \approx 10.6/\delta \approx 106$ MHz. Therefore, real bandwidth economy for the proposed modulation mode is about fivefold.

Interesting, too, is to see how fruitful it might be to implement such a modulation mode as the BOC(10,5) chosen for the new GPS M-code using MSK. In a general case of BOC(n_m, n_c), the normalized signal power spectrum density is

$$\tilde{G}(f) = \frac{\delta}{2n_p} \left| \frac{\sin 2n_p \pi f \delta}{\pi f \delta} \tan \pi f \delta \right|^2 \quad (3)$$

where $n_p = n_m/n_c$ – number of meander periods per BOC chip. If BOC is MSK-converted, i.e., the meander is replaced by its first harmonic, then the normalized power spectrum density of such a BOC-MSK(n_m/n_c) signal becomes

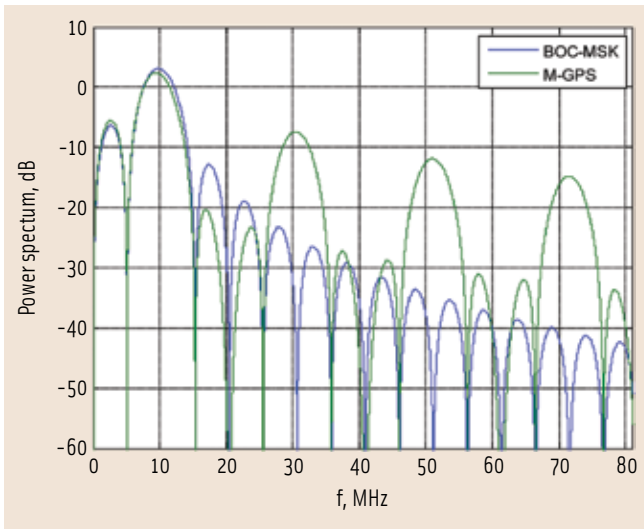


FIGURE 4 Power spectra of BOC(10,5) and BOC-MSK(10,5) signals

$$\tilde{G}(f) = \frac{4\delta}{\pi^2 n_p} \left| \frac{\sin 2n_p \pi f \delta}{1 - (2f\delta)^2} \right|^2 \quad (4)$$

For $n_p = 10$, $n_c = 5$ these spectral densities are presented in Figure 4. As can be seen, an MSK-converted BOC(10,5) has a far higher spectral efficiency compared to the conventional BOC(10,5). For instance, at a distance from the carrier of about 40 megahertz or more, the former has spectral lobes at least 20 decibels lower than the latter. Translated to terms of 99 percent bandwidth, this means that for the BOC-MSK(n_m/n_c), as soon as $n_p \geq 2$, $W_{0.99} \leq 2.1/\delta$. For a conventional BOC(10,5), the analogous figure is $W_{0.99} \approx 18/\delta$, which is 8.6 times wider compared to the previous value.

Potential Accuracy of MSK Ranging

Our suggested signal gains spectral compactness compared to legacy modulations as a result of the smoothness of MSK chip. Theoretically, we pay for this compaction in the form of a degradation of the potential measurement accuracy of pseudoranges or, equivalently, the time of arrival (TOA), τ , of the satellite ranging code against the local time scale.

In practical calculations, however, we should allow for the finite bandwidth of both the transmitter and receiver and, if some realistic assumption are made on this account, the accuracy of time measurement of the proposed signals appears to be no worse than with the existing ones. Indeed, we can readily show that the additive white gaussian noise (AWGN) variance $\text{var}\{\hat{\tau}\}$ of the TOA estimate $\hat{\tau}$ for a BPSK signal with chip duration Δ is given by this version of the Woodward formula

$$\text{var}\{\hat{\tau}\} \approx \Delta^2 \left[q^2 4W\Delta \left(1 - \frac{\sin 2\pi W\Delta}{2\pi W\Delta} \right) \right]^{-1} \quad (5)$$

where $q \gg 1$ is the accumulated SNR at the estimator input and $2W$ is the bandwidth of receiver frequency-selective circuits.

In the alternative case of a narrowband chip of the same duration Δ built as a series of n_n δ -duration MSK-microchips,

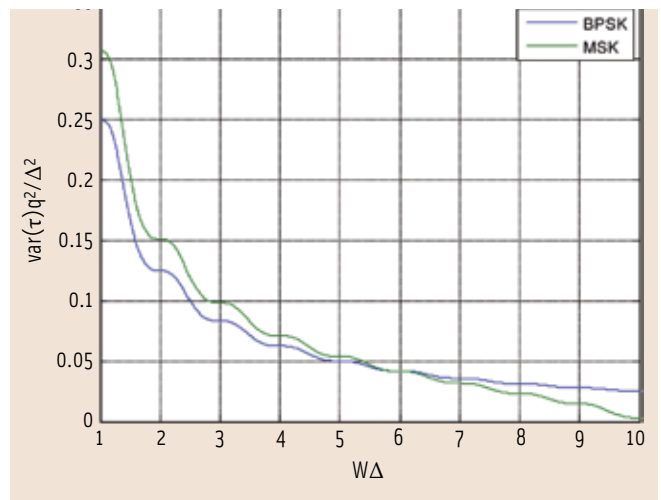


FIGURE 5 Variance of time of arrival estimate versus receiver bandwidth (civil signal)

the variance of τ -estimate is found to be

$$\text{var}\{\hat{\tau}\} \approx \frac{\Delta^2}{64q^2 F_2 \left(n_n, \frac{W\Delta}{n_n}, 0 \right)} \quad (6)$$

where

$$F_2(n, u, v) = n \int_0^u \left[\frac{x \sin n\pi x}{(1 - 4x^2) \tan \pi x} \right]^2 \cos(2n\pi vx) dx$$

First of all, let us use the foregoing equations to assess the accuracy of measuring TOA provided by the proposed narrowband signal in comparison with the C/A code. To do that we have to make $\Delta = \Delta_n = 1/f_c$. Assuming also, as earlier, $n_n = 10$, we make microchip length δ equal to the P-code chip duration (about 100 nanoseconds). The curves of the normalized τ -estimate variances, $\text{var}\{\hat{\tau}\}q^2/\Delta^2$, for both a rectangular chip and the one composed of $n_n = 10$ MSK microchips are presented in Figure 5 against a normalized receiver half-bandwidth $W\Delta$.

Although for a relatively narrow band $W\Delta < 6$ the MSK-composed narrowband chip slightly yields (less than 11 percent) to the rectangular one in the standard deviation of TOA estimate, with the bandwidth widened the pattern becomes completely opposite. When the bandwidth $2W = 20 / \Delta \approx 20$ MHz, the standard deviation of a TOA estimate with the proposed chip becomes more than three times lower against what is typical of the legacy one.

This latter phenomenon is explainable by the presence of the frequency $1/\delta$ harmonic in the MSK-composed chip that, being passed by the wideband receiver, contributes to the increase of τ -measuring accuracy. The effect thereby obtained is the same as takes place with multiplexed BOC (MBOC) or time-multiplexed BOC (TMBOC) modulations (see, for example, the referenced article by G. Hein *et alia* in Additional Resources), but unlike them is gained automatically, without inserting additional “fast” signal components.

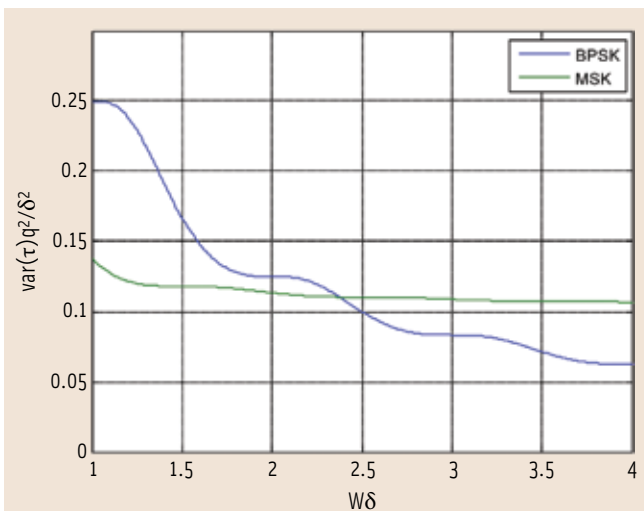


FIGURE 6 Variance of TOA estimate versus receiver bandwidth (wideband signal)

Now let us pass on to the wideband signal and compare the accuracy of its proposed versions with the one of a legacy P-code. If the new signal chip is a microchip itself, then in the equations (5)–(6) we need only make $\Delta = \delta$ and $n_n = 1$. Figure 6 gives the curves of normalized variances thus obtained.

As can be seen, as long as the receiver bandwidth is narrower than $5/\delta \approx 50$ MHz the smoothed chip provides an accuracy gain versus a legacy one, and its tangibility (less than 40 percent in standard deviation) loss is observed only when the bandwidth is nearing 80 megahertz. Of course, we can hardly treat as realistic this large a value of a receiver bandwidth. For example, in the book by P. Groves referenced in the Additional Resources section the transmission bandwidth of any GPS signal, which is simultaneously the maximum useful receiver bandwidth, is stated to be 30.69 megahertz.

With these factors in mind, we can conclude that, assuming plausible values for the receiver bandwidth, the MSK signal format in no way provides poorer performance in ranging accuracy compared to legacy signals.

Multipath Resistance

The issue of multipath resistance is among the most critical in designing GNSS signals and, again, at first glance it might seem that multipath performance of a smoothed chip is poorer than with a rectangular one. Nevertheless, in line with the previous section when the real receiver frequency selectivity is taken into consideration, an MSK-based signal appears completely competitive with the legacy ones.

In numerous sources, assessment of the multipath influence is demonstrated employing a graph of the code-tracking error envelope. Curves thus built depend critically on the discriminator type, strobe spacing, and strobe length, and for every possible chip shape these factors should be adjusted individually to optimize performance.

In this section we will follow an alternative approach that concentrates on the potential accuracy of measuring TOA of the line-of-sight signal distorted by multipath interference. By

this means, we will find out to what extent the multipath is destructive in principle when applied to both traditional signals and our proposed modulation technique.

Operating as before with the signal baseband equivalents, we assume the model of the multipath interference as a single replica of the line-of-sight signal scaled by a and lagging behind by delay θ . In the most plausible scenario we have to treat a and θ as unknown “nuisance” parameters that obstruct measurement of the useful parameter: signal TOA τ .

A universal strategy to handle nuisance unknowns when their a priori statistics are unavailable is to include them in the list of measured quantities, omitting their estimates after they are obtained. Thus, we come to the 3D vector (τ, θ, a) to be estimated from the observed mixture of the useful signal and multipath. Variances of estimates of its components are asymptotically (under large SNR) equal to the diagonal elements of the inverse Fisher matrix (see, e.g., the monograph by H. Van Trees referenced in Additional Resources). Specifically interesting to us is the variance of estimate $\hat{\tau}$ of the signal TOA after calculating size-three Fisher matrix elements, and the matrix inversion is found to be

$$\text{var}_{mp}\{\hat{\tau}\} = \frac{\text{var}\{\hat{\tau}\}}{1 + \frac{[\rho'(\theta)]^2}{\rho''(0)} - \left[\frac{\rho''(\theta)}{\rho''(0)}\right]^2} \quad (7)$$

where the subscript in $\text{var}_{mp}\{\hat{\tau}\}$ stresses that this variance is calculated allowing for multipath, $\text{var}\{\hat{\tau}\}$ is the variance in absence of multipath (equations (5), (6)), θ is a genuine value of multipath delay relative to the useful signal, and $\rho(\tau)$ is the normalized signal autocorrelation.

To simplify the equations to come, let us suppose that the receiver passband W is bound by the non-rigorous condition with a chip duration Δ : $W\Delta = k$ with k integer. For instance, in the case of rectangular chips this means that the receiver filter passes through an integer number of signal spectral lobes. Then, for a legacy (BPSK) GPS signal with chip duration Δ , the following expressions can be derived

$$\frac{[\rho'(\theta)]^2}{\rho''(0)} = -\frac{1}{8k\pi \text{Si}(2k\pi)} \left\{ \text{Si}\left[2k\pi\left(1 + \frac{\theta}{\Delta}\right)\right] - \text{Si}\left[2k\pi\left(1 - \frac{\theta}{\Delta}\right)\right] - 2\text{Si}\left(2k\pi\frac{\theta}{\Delta}\right) \right\}^2 \quad (8)$$

and

$$\frac{\rho''(\theta)}{\rho''(0)} = \frac{\sin\left(2k\pi\frac{\theta}{\Delta}\right)}{2k\pi\frac{\theta}{\Delta}} \cdot \frac{1}{1 - \left(\frac{\theta}{\Delta}\right)^2} \quad (9)$$

with $\text{Si}(\cdot)$ being the integral sine.

On the other hand, for a suggested narrowband Δ -duration chip formed by repetition of the n_n MSK-microchips, a routine but somewhat tedious mathematical manipulation results in

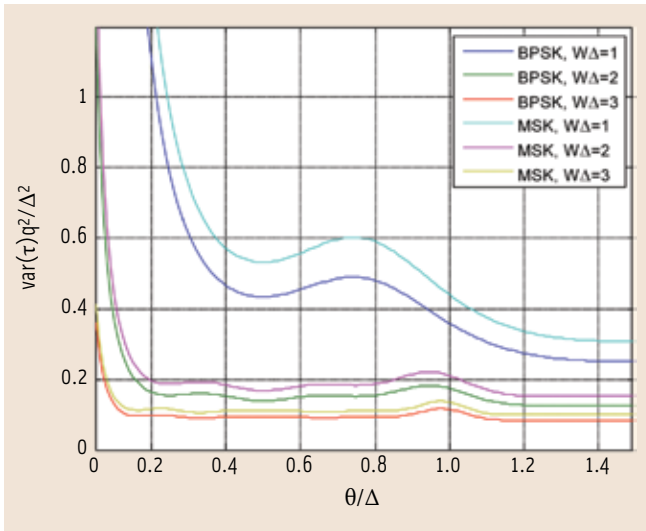


FIGURE 7 Variance of TOA estimate versus multipath delay, civil signal

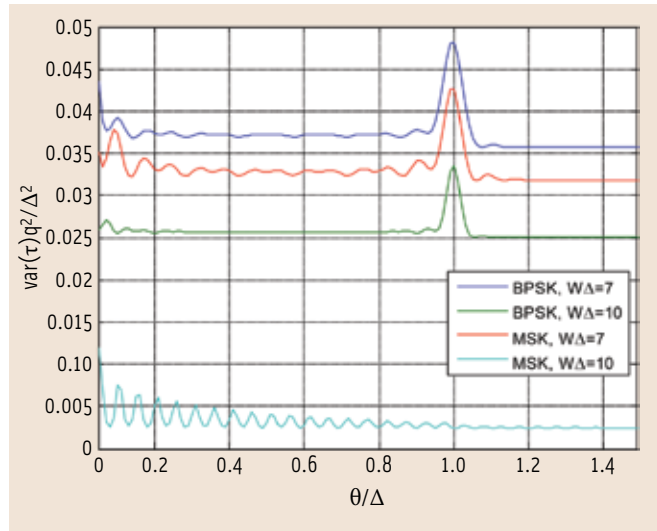


FIGURE 8 Variance of TOA estimate versus multipath delay, civil signal

$$\frac{[\rho'(\theta)]^2}{\rho''(0)} = \frac{\left[F_1\left(n_n, \frac{W\Delta}{n_n}, \frac{\theta}{\Delta}\right) \right]^2}{F_2\left(n_n, \frac{W\Delta}{n_n}, 0\right) F_0\left(n_n, \frac{W\Delta}{n_n}\right)} \quad (10)$$

$$\frac{\rho''(\theta)}{\rho''(0)} = \frac{F_2\left(n_n, \frac{W\Delta}{n_n}, \frac{\theta}{\Delta}\right)}{F_2\left(n_n, \frac{W\Delta}{n_n}, 0\right)} \quad (11)$$

where

$$F_1(n, u, v) = \frac{4}{\pi} \int_0^u x \left[\frac{\sin \pi \pi x}{(1 - 4x^2) \tan(\pi x)} \right]^2 \sin(2n\pi v x) dx$$

and

$$F_0(n, u) = \frac{16}{n\pi^2} \int_0^u \left[\frac{\sin \pi \pi x}{(1 - 4x^2) \tan(\pi x)} \right]^2 dx$$

Figure 7 and Figure 8 show dependencies of variance of the TOA estimate on multipath delay θ normalized to a chip duration Δ for the proposed narrowband or civil signal. They are built based on equations (7)–(11) and (5)–(6) under the assumption $\Delta = \Delta_n = 1/f_c$ and $n = n_n = 10$ to correspond to the chip duration of C/A code and its ratio to the that of the P-code.

As can be clearly seen, for a narrow receiver band ($W\Delta \leq 3$) the legacy chip provides slightly higher accuracy (within 10 percent as for the standard deviation) of the TOA estimate, while with bandwidth widening the pattern changes crucially in favor of the chip composed of MSK-microchips. For example, when the receiver bandwidth approaches 20 megahertz, the MSK-based chip excels the rectangular one in TOA estimate standard deviation by about three times.

The physical reason for this has already been clarified: the harmonic of frequency $1/\delta$ present in the MSK-composed chip and passed by the wideband receiver perceptibly improves the

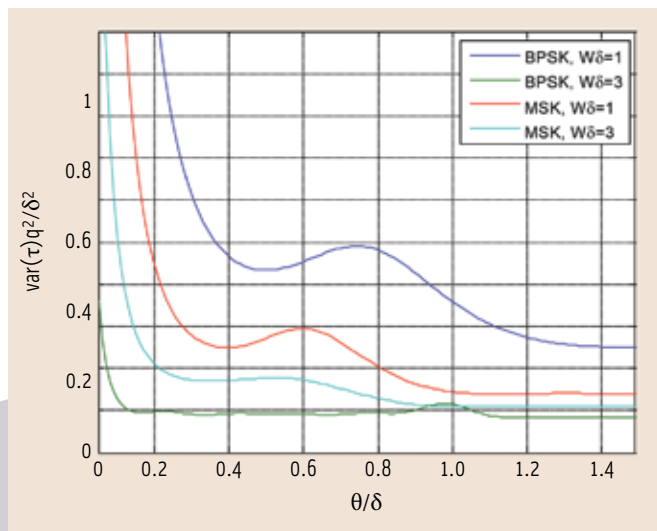


FIGURE 9 Variance of TOA estimate versus multipath delay, wideband signal

performance of measured TOA. An important note: from Figures 7–8 we can see that for both signal types, whenever receiver bandwidth is about $4/\Delta$ (4 MHz) or wider, a lagging of the multipath relative to the direct signal of more than 0.2 chip duration does not materially affect the potential TOA estimate accuracy.

Figure 9 presents analogous curves for the wideband signals obtained from the same equations after substituting $\Delta = \delta$ and $n = 1$. As with the scenario without multipath, when the receiver bandwidth is moderate $W\delta \leq 2$ (40 megahertz), the TOA estimate with MSK is remarkably more precise compared to the legacy modulation; only for $W\delta \geq 3$ (60 megahertz) does the latter type of signal do better. But even under such a (hardly realistic) scenario of receiver bandwidth, loss in accuracy of the MSK chip in terms of estimated standard deviation is never more than 35 percent compared to the legacy signal as long as multipath delay exceeds 0.2 chip duration.

Conclusions

The following statements may briefly summarize our discussion:

- The MSK modulation and, in general, spectral-efficient modulation formats provide a productive tool for frequency coordination between the neighboring systems in the RF spectrum, particularly for mitigating the problem of penetration of GNSS emissions into the radio astronomy band.
- Within the MSK modulation mode the task of aggregating two sorts of signals: the narrowband (civil) and wideband ones can be feasibly solved by composing the narrowband chip as a series of short microchips.
- The potential accuracy of measuring TOA with the proposed MSK signals is either comparable or even better relative to the legacy signals as soon as realistic values of receiver bandwidth are taken into account.
- The same is true for the potential multipath resistance defined by the accuracy of the TOA estimate in the presence of multipath with a priori unknown delay and intensity.
- There is no need to reproduce an exact narrowband chip shape in a cheap commercial receiver: its replacement by a plain rectangle will lead to the energy loss within only 0.9 decibel.
- The analysis presented here is just a first step limited to the MSK format only. With an optimized microchip, we can expect to achieve even better performance.

Additional Resources

- [1] Avila-Rodriguez, J.-A., and S. Wallner, J.-H. Won, B. Eissfeller, A. Schmitz-Peiffer, J.-J. Floch, E. Colzy, and J.-L. Guerin, "Study on a Galileo Signal and Service Plan for C-Band," *Proceedings of GNSS 2008*, Toulouse, France, April 22–25, 2008
- [2] Groves, P., *Principles of GNSS, Inertial, and Multisensor Integrated Navigation Systems*, Artech House, 2008
- [3] Hein, G., and J. Betz, A. Pratt, A.R., L. Lenahan, J. Owen, J., J.-L. Issler, and T. Stansell, "MBOC: The New Optimized Spreading Modulation Recommended for Galileo L105 and GPS L1C," *Inside GNSS*, Vol.1, No. 4, pp. 57–65, May/June 2006
- [4] Ipatov, V., and B. Shebshaeich, "GLONASS CDMA: Some Proposals on Signal Formats for

Future GNSS Air Interface, *Inside GNSS*, Vol. 5, No. 5, pp. 46–51, July/August 2010

[5] Proakis, J., *Digital Communications*, McGraw Hill, N.Y., 2001

[6] Schmitz-Peiffer, A., and A. Fernández, B. Eissfeller, B. Lankl, E. Colzy, J.-J. Floch, J.-H. Won, J.-A. Avila-Rodriguez, F. Stopfkuchen, M. Anghileri, O. Balbach, R. Jorgensen, S. Wallner, and T. Schüler, "Architecture for a Future C-band/L-band GNSS Mission. Part 2: Signal Considerations and Related User Terminal Aspects," *Inside GNSS*, Vol. 4, No. 4, pp. 52–63, July/August 2009

[7] Sklar, B. *Digital Communications*. Prentice-Hall, Upper Saddle River, NJ, 2001

[8] Van Trees, H., *Detection, Estimation and Modulation Theory, Part 1*, John Wiley & Sons, 2001

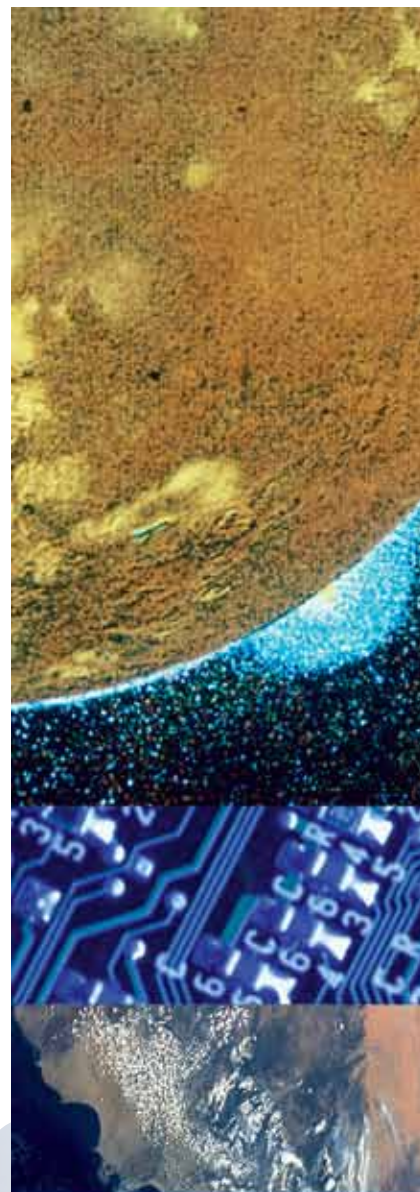
Authors



Valery P. Ipatov graduated from Leningrad Electrotechnical Institute (now St. Petersburg State Electrotechnical University "LETI") with the diploma of engineer in radio technology where he later received the candidate of science and doctor of science degrees in the field of radar and navigation. Since 1964 he had been with LETI as a researcher, postgraduate student, assistant professor, associate professor, professor and head of department. From 2001 to 2007 he was a Professor of telecommunications at the University of Turku, Finland, keeping simultaneously professor's chair at LETI. His research interests are in the area of spread spectrum, discrete signal design, communication theory, coding, statistical signal processing, satellite radio navigation. He is the author of a number of books, including *Spread Spectrum and CDMA. Principles and Applications* (Wiley & Sons, Chichester, 2005).



Boris V. Shebshaeich graduated from Leningrad Electrotechnical Institute (now St. Petersburg State Electrotechnical University "LETI") as an engineer in radio technology and since 1975 has permanently been with Russian Institute of Radionavigation and Time. There he has progressively passed positions from junior researcher to CEO and chief designer and has been awarded the candidate of science degree in radar and navigation. His R&D activities cover ground- and space-based radionavigation, navigation air interface and user equipment design, and future GNSS philosophy. He was distinguished by the Russian Academy of Science and GLONASS-Forum Association for contributions to positioning, navigation, and timing (PNT) technologies and GLONASS development. 



There's more!

web news
digital edition
e-newsletter

insidegnss.com